Activation of *n*-pentane while prolonging HZSM-5 catalyst lifetime during its combined reaction with methanol or dimethyl ether

Tomás Cordero-Lanzac[1,*], Cristina Martínez[2], Andrés T. Aguayo [1], Pedro Castaño[1,3], Javier Bilbao[1], Avelino Corma[2]

[1] *Department of Chemical Engineering, University of the Basque Country (UPV/EHU), PO Box 644, 48040, Bilbao, Spain*

[2] *Instituto de Tecnología Química, Universitat Politècnica de València-Consejo Superior de Investigaciones Científicas (UPV-CSIC), Avenida de los Naranjos s/n, 46022 Valencia, Spain*

[3] *King Abdullah University of Science and Technology, KAUST Catalysis Center, Multiscale Reaction Engineering, Thuwal, 23955-6900, Saudi Arabia*

Corresponding author: tomas.cordero@ehu.eus

ABSTRACT

This work explores the synergies during combined reactions of *n*-pentane (nC_5) with oxygenates (methanol or dimethyl ether, OX). The experimental runs have been carried out in a packed bed reactor at 500 ºC, using a high silica HZSM-5 zeolite-based catalyst with different oxygenate-to-*n*-pentane (OX/nC_5) ratios in the feed. A significant enhancement of the *n*-pentane conversion occurs for low OX/nC_5 ratios in the feed (0.1-0.25), especially when using dimethyl ether (DME). In addition, the presence of *n*-pentane reduces the rate of catalyst deactivation by coking during the conversion of oxygenates. These results have been explained on the grounds of a mechanistic interaction between the reactants: (1) the fast formation of methoxy and olefin intermediates from oxygenates, particularly from DME, could explain the promotion of *n*-pentane cracking, by facilitating the activation of the alkane by hydrogen transfer reactions; (2) the attenuation of deactivation during the conversion of oxygenates could be related to a lower extent of the arene cycle in the dual-cycle mechanism (limiting the polymethylbenzene formation). The analyses of used catalysts by means of temperature-programmed oxidation and confocal fluorescence microscopy have pointed out the higher reactivity of DME than that of methanol also for yielding coke structures.

Keywords: olefins; HZSM-5 zeolite; catalytic cracking; dual-cycle mechanism; deactivation; coke

1. Introduction

The catalytic cracking of paraffins is one of the most studied alternatives for producing olefins from the naphtha cut of the refineries (C_{5-12}) [1], because it has lower energy requirement and higher propylene selectivity than those of the steam/thermal cracking [2]. Catalytic cracking is carried out over acid microporous sieves, being HZSM-5 zeolite the most studied due to its shape selectivity that maximizes the olefin production. Promising and encouraging results have been reported in the cracking of paraffins of relatively long carbon chains, such as C_{6-10} [3–5]. Nonetheless, the lightest paraffins contained in the naphtha (C_5) or in gaseous fractions (C_{1-4}) are much more difficult to crack [6]. High temperatures are recommended for promoting cracking but avoiding side reactions [7]. Steam catalytic cracking (SCC) has also been proposed for naphtha processing with enhanced selectivity to ethylene and propylene in the presence of water and high temperatures (up to 700 ºC) [8]. However, the high temperature and presence of steam could also lead to an irreversible deactivation of zeolites by dealumination, with the corresponding increase of the catalyst makeup [9].

Within the possible process modifications for activating light paraffins and promoting a selective cracking to light olefins, Martin et al. [10,11] proposed the so-called coupled methanol and hydrocarbon cracking (CMHC). The first goal was to take advantage of the exothermic character of the methanol-to-olefins (MTO) process in order to overcome the energetic requirements of the catalytic cracking. The synergies between both reactions were also previously observed for a feed mixture of n-butane/methanol in the temperature range of 500-550 ºC and low space time values [12]. The clearest evidences of C-C paraffinic bond activation using methanol were reported by Yu et al. [13] in experiments with propane and labeled carbon reactants. They saturated the HZSM-5 zeolite with labeled methoxy species at very controlled conditions and made them to react directly with propane, which confirmed a promoted hydride transfer pathway between both species. The combined reactions of paraffins and methanol were studied aiming for the intensification of propylene in the methanol-to-propylene (MTP) process. A significant enhancement of its yield was reported by co-feeding *i*-butane at 470-500 ºC and full conversion of methanol [14]. Likewise, a positive synergy was found when the C_{4-6} hydrocarbon byproducts were recirculated in the MTO process [15].

Coupling the reactions of paraffins and methanol means the coexistence of the two well-established mechanisms on the same acid sites of the HZSM-5 zeolite: the carbocationic mechanism of paraffin cracking [16–18] and the dual-cycle mechanism of MTO [19]. Chang et al. [20] related both mechanisms in combined reactions and suggested a faster route for the catalytic cracking of *n*-hexane due to the formation of intermediates from methanol. On the one hand, paraffin cracking mechanism follows a pathway involving the monomolecular cracking (via penta-coordinated carbonium ions that evolve towards light paraffins), the bimolecular cracking (via hydride transfer between the paraffin and an adsorbed carbenium ions) and the oligomerization-cracking (toward higher hydrocarbons and finally coke) [16,21,22]. On the other hand, in the dual-cycle mechanism of oxygenates, the methylation/*β*-scission of the olefin primary products (alkene cycle) is coupled with the methylation/dealkylation of methylbenzenes (arene cycle) through hydrogen transfer and cyclization pathways [19,23,24]. In this case, the formation of coke takes place from two different stages [25,26]: (i) the evolution of methylbenzene intermediates towards polyaromatic structures of coke and (ii) the olefin cyclization and condensation, which requires a high development of the first stage. Then, the acid properties (density and strength of the sites) and topology of the catalyst have a strong influence on the extent of each stage [27,28]. In this regard, HZSM-5 zeolite favors the diffusion of these methylbenzenes, thus allowing the two stages of coke formation to be distinguished [26].

Traditionally, dimethyl ether (DME) has been considered in thermodynamic equilibrium with methanol, assuming similar reactivities for both in the MTO process. Nonetheless, different studies have demonstrated that DME is more reactive than methanol [29]. Indeed, in-situ IR measurements pointed out its faster ability to form methoxy species, attributed to its higher affinity towards the Brønsted acid sites [30,31]. Despite the discrepancies in the literature about the formation of the first C-C bond, Li et al. [32] reported that DME reacts faster than methanol with methoxy species, forming methoxy-methyl cation intermediates. Moreover, this is applicable to the reaction of methoxy species from DME with other hydrocarbons, as was observed for the methylation of benzene [33]. The reactivity of DME presents a renewed interest in the context of its transformation into olefins (DTO, dimethyl ether-to-olefins process) [34].

In this work, we have analyzed the combined reactions of *n*-pentane with methanol or DME, comparing the reactivity of both oxygenates. Our aim is to progress towards the

understanding of the advantages of co-feeding paraffins (*n*-pentane) and oxygenates, linking the mechanisms that drive their individual reactions. For this, a catalyst based on a high silica HZSM-5 zeolite embedded in a mesoporous matrix of γ-Al_2O_3 has been used. The benefits of coupling paraffin and oxygenate conversions on the activation of the *n*-pentane (selected as the lightest and less reactive compound in naphtha) and on the attenuation of coke formation from oxygenates have been studied by comparing the reactivity of individual and combined reactions in a packed bed continuous reactor at 500 ºC. The effect of the oxygenate-to-paraffin ratio in the feed on conversion, product distribution and on their evolution with time on stream is discussed.

2. Experimental

2.1. Catalyst preparation

HZSM-5 zeolite-based catalyst was synthesized by an agglomeration procedure using pseudoboehmite (Sasol Germany) as a binder and a colloidal dispersion of α-Al_2O_3 (Alfa Aesar, 22 wt %) as inert filler (30 and 20 wt% in the final catalyst, respectively). The commercial zeolite (Zeolyst International) with a Si/Al ratio of 140 was homogeneously mixed with the other components and then, extrudates of the resulting slurry were prepared. These extrudates were dried at room temperature for 12 h and afterwards at 110 ºC in a vacuum-dryer for 2 h. The agglomerates were sieved to a catalyst particle size between 0.125 and 0.3 mm and then calcined at 575 ºC for 2 h, reaching the final temperature at a heating rate of 5 ºC min^{-1}. During the thermal treatment, pseudoboehmite is converted into a mesoporous γ-Al_2O_3.

The selection of the HZSM-5 zeolite with high Si/Al ratio was motivated by the purpose of reducing the catalyst acid site density. In this way low *n*-pentane conversions were attained, which enabled quantifying the effect of co-feeding methanol and DME. In addition, we aim at reaction conditions and catalyst properties that minimize the extent of the arene cycle during the transformation of oxygenates [35]. The agglomeration of the zeolite provides the catalyst particles with the required mechanical resistance, as well as with a porous structure that favors the diffusion of coke precursors outside the zeolite channels [34].

2.2. Catalysts characterization

The porous texture of the fresh and used catalysts was characterized by means of N_2 adsorption-desorption isotherms at -196 ºC in a Micromeritics ASAP 2010 apparatus. From the isotherms, the specific surface area was calculated using the BET equation (S_{BET}), the micropore volume (V_{micr}) and external surface area (S_{ext}) were calculated by applying the *t*-plot method and the mesopores volume (V_{mes}) was estimated by difference with the total adsorbed volume during the experiments.

The acidity of the catalyst was estimated through adsorption-desorption of the base-probe molecule *tert*-butylamine (tBA), in a Setaram TG-DSC calorimeter. Samples were pretreated at 550 ºC in He for 2 h before the adsorption of tBA, which was carried out at 100 ºC. After saturation, physisorbed tBA was swept with He and then, a temperature-programmed desorption was carried out, raising the temperature up to 500 ºC using a heating rate of 5 ºC min^{-1}. The calorimeter was coupled to a mass spectrometer in which the signal of butene was monitored (m/z = 56). Butene is the main product of tBA cracking during the TPD experiments, and therefore these experiments allow for measuring the hydrocarbons cracking capability exhibited by the catalysts.

Table S1 shows the main textural parameters and total acidity of the zeolite and the fresh catalyst. As expected, the dilution of the zeolite in the mesoporous matrix leads to a decrease in the S_{BET} surface area and total acidity, whereas the mesopore volume and external surface of the catalyst are higher than those of the zeolite.

The amount, nature and location of coke on the used catalysts were measured by thermogravimetric analysis during temperature-programmed oxidation experiments (TG-TPO) in a TGA Q5000 IR thermobalance from TA Instruments. Prior to the analyses, samples were submitted to a sweeping stage in N_2 during 30 min at the reaction temperature in order to remove the adsorbed species within the catalyst pores. After cooling the sample down to room temperature, the TPO experiments were performed in air by raising the temperature up to 550 ºC at a temperature rate of 5 ºC min^{-1}, and maintaining it isothermal during 2 h.

The morphology of the used catalysts was studied by confocal fluorescence microscopy (CFM) in a ZEISS LSM 800 Microscope, provided with a turbo pumped chamber, a motorized stage and multialkali, GaAsP and Airyscan detectors. The microscope is also provided with three excitation channels with diode lasers at 405, 488 and 561 nm, making the samples emit fluorescence in the wavelength of blue, green and red ranges,

respectively. The used accelerating voltage was 20 kV. Brightness and contrast were equally set for all samples in order to compare the intensity of emitted fluorescence with the surface concentration. Images were formed by stacking 10-20 raw images samples of different *z* axis corresponding to 0–50 μm deep on the particle surface. Reflection images of the samples were also obtained, for which particles were submitted only to the 405 nm laser and the reflected beam was collected by the detector.

2.3. Experimental runs

Experimental runs of *n*-pentane (nC_5) catalytic cracking, methanol (MeOH) and dimethyl ether (DME) conversion, as well as the combined reactions of nC_5 and oxygenates, were carried out in a stainless steel packed bed reactor (PID & Tech) heated by a cylindrical ceramic oven. The equipment was provided with mass flow controllers for feeding inert gases and DME, a HPLC pump (Gilson) for feeding MeOH and a syringe pump (up to 100 mL of maximum volume, Hardvard) for feeding nC_5. Catalyst particles were mixed with inert SiC with a sieved particle size of 0.5–0.6 mm in order to ensure isothermal conditions and a constant catalytic bed height during the experiments. Before reactions, the catalyst was submitted to a pretreatment at 550 ºC during 2 h in a continuous flow of air for sweeping water and possible impurities located within the zeolite pores. The reactions were carried out using the following conditions: 500 ºC; total pressure of 1.5 bar; space time of 1.0 $g_{catalyst}$ h mol_C^{-1} and time on stream up to 15 h. The partial pressure of the C-containing reactants was 1.0 bar (diluted in N_2) in both individual and combined reactions. Different mixtures of oxygenates and nC_5 were used in the combined reactions. The used oxygenate-to-nC_5 molar ratios (OX/nC_5) were 0.1, 0.25 and 1. The flow rates of the reactants were set and the N_2 flow rate and catalyst weight were varied in each reaction in order to perform the runs with the same space time (in contained C units) and partial pressure of C-containing reactants.

The reactor was connected to a gas chromatograph (Agilent 3000A MicroGC) for the on-line identification of the reaction products. The gas chromatograph was provided with four columns in which the following products are identified: (i) MS-5 column, CH_4 and CO; (ii) Porapak Q column, CO_2, DME and water; (iii) Al_2O_3 column, $C_{2–5}$ paraffins and olefins; (iv) Stabilwax column, $C_{6–8}$ hydrocarbons, methanol and BTX aromatics. Experimental runs were monitored by following different reaction indexes (conversion, selectivity and yields), whose definitions and equations are detailed in **Table S2**. Three runs of all experiments were performed in order to ensure

reproducibility. The relative error in all cases was lower than 3%, applied to all figures of the manuscript.

3. Results and discussion

The results of combined reactions of *n*-pentane (nC_5) with methanol (MeOH) or dimethyl ether (DME) are compared with those of the individual reactants. First, an evaluation of the synergetic effect that leads to the activation of nC_5 is made (section 3.1), followed by a study of the attenuation of catalyst deactivation by coking from oxygenates (section 3.2). These effects are discussed based on the proposed mechanism for each reaction, the relation between both of them and the deposition of coke.

3.1. Activation of n-pentane catalytic cracking by oxygenates

Figure 1 shows the initial nC_5 conversion when MeOH or DME were co-fed with different molar OX/nC_5 ratios at 500 ºC and a space time of 1.0 $g_{catalyst}$ h mol_C^{-1}. Under these conditions, the individual reaction of nC_5 shows a conversion of ca. 7%. This nC_5 conversion increases up to ca. 9.5 and 8.5% for $MeOH/nC_5$ molar ratios of 0.1 and 0.25, respectively. However, the use of a MeOH/nC5 ratio of 1 leads to a decrease in the nC_5 conversion to values of ca. 4%. When DME is co-fed with DME/nC_5 ratios of 0.1 and 0.25, the increase in the achieved nC_5 conversion is higher than those obtained with MeOH. A small improvement of the nC_5 conversion is even observed with a feed consisting of a DME/nC_5 ratio of 1. These results are attributed to the catalytic conversion of nC_5 and not to thermal or matrix effects. In a previous experiment with the mesoporous matrix but without zeolite at this temperature (not shown in **Figure 1**), a negligible nC_5 conversion was observed (< 1%) with non-significant production of olefins.

Initial nC_5 reaction rates can be calculated from the low conversion values, considering the weight hour space velocity (WHSV) of nC_5 (**Eq. S5** in **Table S2**). **Figure S1** depicts the corresponding values of nC_5 reaction rate for the experiments in **Figure 1**. The enhancement of nC_5 reactivity is evidenced when co-feeding OX/nC_5 ratios of 0.1 and 0.25. The trend is similar to that observed in terms of nC_5 conversion, with a better improvement of the nC_5 reaction rate in the case of DME. Nonetheless, the rate of the paraffin reaction is not improved with any of the oxygenates at OX/nC_5 ratio of 1.

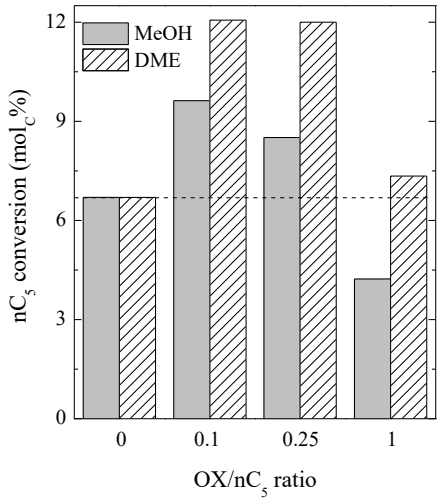

Figure 1. Effect of co-feeding different MeOH/nC_5 and DME/nC_5 ratios on the initial nC_5 conversion (500 ºC, 1.0 $g_{catalyst}$ h mol_C^{-1})

The reaction mechanism of *n*-paraffin cracking catalyzed by acid zeolites has been thoroughly studied [18]. It is generally accepted that the sites involved are the Brønsted acid sites of the zeolite and the intermediates are carbenium and carbonium ions. In the absence of more reactive olefins in the feed, the initial activation of the alkane occurs by the protonation of its C-H or C-C bonds and involves the formation of a penta-coordinated carbonium ion [6,36]. In a second step, a carbenium ion is formed by dehydrogenation or by protolytic cracking of the absorbed carbonium, yielding H_2 or a smaller paraffin, respectively. The formed carbenium ions may participate in the propagation step by hydride transfer with the feed molecules and further reaction of the new formed carbenium ions. It can also desorb as an olefin, thus restoring the original Brønsted acid site in a final termination step. Under conditions of high temperature, low alkane partial pressures and/or low alkane conversions, the desorption of the carbenium ion as an olefin is favored over hydrogen transfer reactions [16] and olefin to paraffin molar ratios close to 1 could be expected. This is indeed the case in the individual reaction of nC_5, in which the overall olefin-to-paraffin (O/P, defined in **Eq. S10** in **Table S2**), ethylene-to-ethane and propylene-to-propane ratios are close to one (**Table S3**). The activation of the paraffin on a Brønsted acid site is a highly demanding step, and the addition of oxygenates could increase its reaction rate [13]. Under our reaction conditions, *n*-pentane cracking rate is increased at low concentrations of the oxygenate

(OX/nC_5 ratio ≤ 0.25, see **Figure S1)**, in good agreement with the observations of paraffin activation made by Chang et al. [20]. The O/P ratios of **Table S3** for the combined reactions also suggest that the product distribution is similar to that obtained in the individual reaction of nC_5. Nevertheless, the O/P ratio is higher when a OX/nC_5 ratio of 1 is used in the feed, being the product distribution comparable to those of the individual reactions of MeOH and DME. This result could indicate that in these cases the reaction mechanism is dominated by the MTO mechanism independently on the presence of nC_5.

We hypothesize that higher concentrations of MeOH or DME favor the interaction of the adsorbed methoxy species with the gas phase oxygenates instead of their reaction with the alkane. In contrast, their presence seems to reduce the activation barrier of *n*-pentane at low partial pressures. Despite the lower concentration of oxygenates in the feed, they will be preferentially adsorbed, due to the lower relative energy of the methoxy species formed in this way as compared to the carbonium ion formed by protonation of the alkane [37,38]. Taking the catalytic cracking mechanism into account, the presence of low amounts of methoxy species derived from the addition of MeOH or DME may be promoting the activation of the paraffin in two ways. On the one hand, the H transfer from a fed alkane to the adsorbed methoxy would lead to a pentenium ion and methane. On the other hand, small amounts of propylene formed by the reaction of the adsorbed methoxy species with gas phase oxygenates would be easily protonated by the Brønsted acid sites forming a propenium ion. In both cases, the carbenium ion formed would initiate the propagation cycle of the cracking mechanism by hydrogen transfer with the *n*-pentane molecules in the feed, as described by Yu et al. [13], as well as possible olefin alkylation-cracking reactions. Under the same conditions, DME has been reported to be more reactive than MeOH due to the formation of methoxy intermediates in higher amount [29,39]. Assuming that the degree of converted nC_5 is related to the methoxy intermediates formed from oxygenates, the higher nC_5 conversion co-feeding DME (**Figure 1**) could be attributed to the faster formation of these intermediates, following any of the two above mentioned routes.

The effect of co-feeding oxygenates on the olefin selectivity is also studied by defining a specific index that allows the quantification of the selectivity to olefins in terms of fed nC_5 (**Eq. S8** in **Table S2**). The increment of the selectivity to each olefin is depicted in **Figure 2** at those conditions previously described for **Figure 1**. As expected, positive

increments are only observed in the cases in which the nC_5 conversion was improved. Interestingly, the increase in the selectivity to olefins is higher using a MeOH/nC_5 ratio of 0.25 in the feed than that using 0.1 (**Figure 2a**) despite the lower nC_5 conversion (**Figure 1**). Nonetheless, the highest increment of the selectivity (especially propylene) is observed when co-feeding a DME/nC_5 ratio of 0.1 (**Figure 2b**), thus coinciding with the highest nC_5 conversion. Taking into account the olefin distribution of the individual reactions in **Figure S2**, the increase in the selectivity to olefins by the presence of oxygenates should lead to higher butenes selectivity, due to possible olefin alkylation-cracking events within the zeolite crystals. However, under the conditions of maximum nC_5 conversion obtained when co-feeding DME in a DME/nC_5 ratio of 0.1, the presence of the oxygenate does not only enhance the nC_5 conversion but propylene is also the main product. This could be explained by a larger contribution of the paraffin to the production of olefins, as the product distribution obtained by cracking pure nC_5 is clearly dominated by propylene (**Figure S2**).

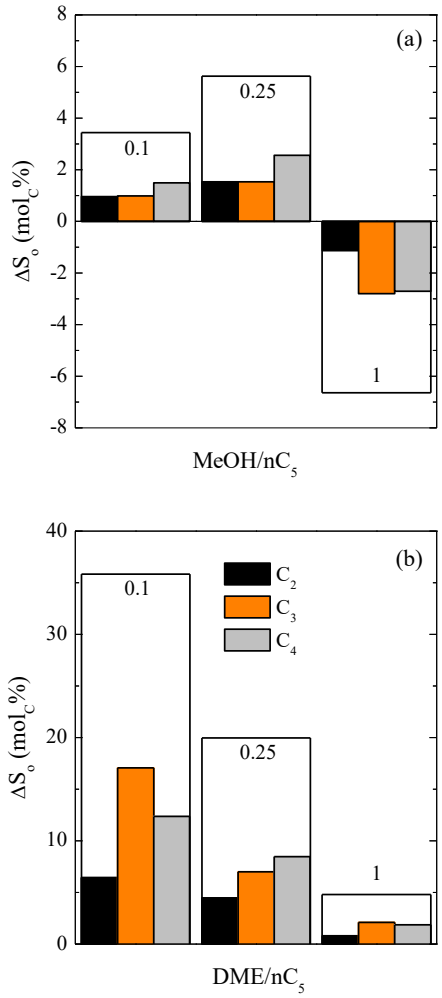

Figure 2. Effect of co-feeding different (a) MeOH/nC_5 and (b) DME/nC_5 ratios on the increments of the total and individual selectivity to olefins in terms of fed nC_5 conversion (500 ºC, 1.0 $g_{catalyst}$ h mol_C^{-1})

3.2. Attenuation of catalyst deactivation and coke deposition in the conversion of oxygenates by n-pentane

Figure 3 shows the evolution with time on stream of the nC_5 and MeOH conversions during the individual and combined reactions using MeOH/nC_5 ratios of 0.1 (**Figure 3a**) and 0.25 (**Figure 3b**) in the feed, the conditions that lead to enhanced nC_5 conversion. In the combined reaction, the overall and nC_5 conversions are stable with time in the studied range, being the alkane conversion values higher in the presence of the MeOH than those obtained when reacting nC_5 alone. Full MeOH conversion is also observed in

all cases during these 6 h runs in the combined reactions, whereas the one in the individual reaction significantly decreases after 3 h on stream.

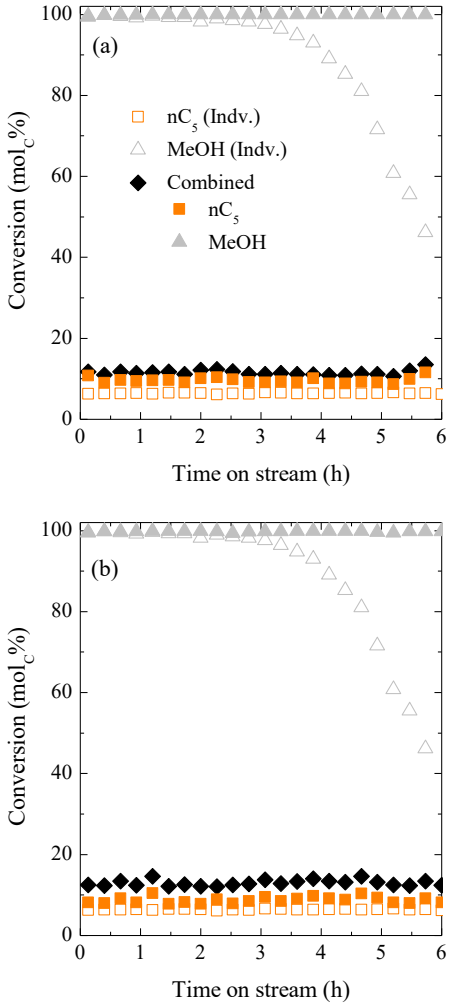

Figure 3. Evolution with time on stream of the overall, nC_5 and MeOH conversions in individual (hollow symbols) and combined reactions (filled symbols) with MeOH/nC_5 ratios of (a) 0.1 and (b) 0.25 (500 ºC, 1.0 $g_{catalyst}$ h mol_C^{-1})

The improvement of the stability of the catalyst observed in the case of the combined reaction with MeOH is more remarkable in the case of DME (**Figure 4**). A drastic activity loss is observed after 2 h of full conversion in the individual reaction of DME. A critical role of formaldehyde in the zeolite deactivation during MTO reaction has been proposed at conditions of low conversion [40]. Nonetheless, at the high used temperature, required for nC_5 cracking, the mechanism of coke formation is probably dominated by the condensation of olefins on the acid sites. And the higher reactivity of

DME as compared to that of methanol [41,42], which implies a high capacity for olefins production, can presumably favor the faster development of coke species. Moreover, the role of water in the attenuation of catalyst deactivation is well-established during the conversion of methanol/DME [43,44], and its concentration is expected to be lower when DME is fed. The reduced diffusion limitations of the HZSM-5 based catalyst could also play a role in this faster catalyst deactivation by coking using DME. Chen et al. [45,46] proved that diffusion limitations using SAPO-34 were more pronounced for DME than for methanol and had a strong influence on the evolution of coke growth. This diffusion limitation with SAPO-34 can explain the observations of Li et al. [47], who reported a faster deactivation when DME was fed.

After 4 h, only CO_x and CH_4 are observed as a consequence of the thermal degradation of DME (ca 15% of conversion). However, full DME conversion is achieved for 6 h when it is co-fed with nC_5, with no apparent catalyst deactivation. Hence, the presence of the alkane in the reaction medium plays a key role in the deactivation rate of the DME conversion (see **Figure 4a** and **4b** for DME/nC_5 ratios of 0.1 and 0.25, respectively). Two synergetic effects can be deduced from the results obtained on these combined reactions of nC_5 with DME. On the one hand, nC_5 conversion increases as compared to its individual reaction and this higher conversion degree is stable during, at least, 6 h on stream. On the other hand, the stability of oxygenate conversions is ostensibly improved, thus shifting from a pronounced activity loss in the absence of nC_5 to an inappreciable deactivation within 6 h on stream in the combined reactions.

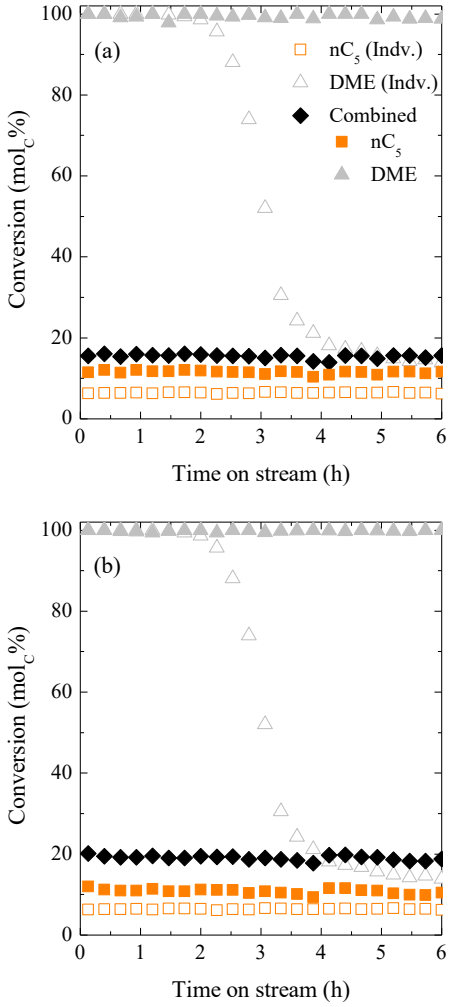

Figure 4. Evolution with time on stream of the overall, nC_5 and DME conversions in individual (hollow symbols) and combined reactions (filled symbols) with DME/nC_5 ratios of (a) 0.1 and (b) 0.25 (500 ºC, 1.0 $g_{catalyst}$ h mol_C^{-1})

The same partial pressure of C-containing reactant in the feed was used for all the experiments described up to now. However, the partial pressure of each reactant is also varied when changing the OX/nC_5 ratio. Reducing the partial pressure of the oxygenate has been reported to decrease the catalyst deactivation rate during its individual conversion into hydrocarbons [39]. Thus, the effect of the reactant dilution with an inert (N_2) was studied in order to discard the role of nC_5 as diluting agent. **Figure S3** depicts the evolution of MeOH (**Figure S3a**) and DME (**Figure S3b**) conversions for three different experiments: individual oxygenate reaction (partial pressure of 1.0 bar), combined reaction of nC_5 and the oxygenate (0.8 and 0.2 bar, respectively) and

individual reaction of the oxygenate (0.2 bar). By diluting the oxygenate with N_2 down to a partial pressure of 0.2 bar, the initial MeOH and DME conversions and the deactivation rate decrease (note the decrease in the conversion decay slope) as a consequence of their lower partial pressure. Especially in the case of DME, the final activity of the catalyst after 6 h is similar for both individual DME reactions despite the differences in the catalyst deactivation profile. Please note that apart from the faster decay of the conversion at the used conditions for the combined reactions, a strict comparison between deactivation rates should not be performed due to the catalyst working at full conversion for MeOH and DME at 1 bar. These results are far from the surprising stability of the oxygenate conversion registered when they were co-fed with nC_5 (**Figures 3** and **4**).

Therefore, the improvement observed when co-feeding nC_5 cannot be only attributed to a dilution effect. The attenuation of catalyst deactivation could be explained by the competitive adsorption of both reactants on the acid sites and by the participation of the paraffin in the dual-cycle mechanism of oxygenates. Regarding this mechanism over HZSM-5 zeolites, many factors such as Si/Al ratio, Al location or crystal size can affect the selectivity and catalyst lifetime [48]. Svelle et al. showed that the hydrocarbon pool mechanism applicable to the MFI porous structure does not involve the highest methylbenzenes (hexa- and heptamethylbenzenes), which are unreactive species and the main responsible for the formation of coke [35]. The continuous methylation of these big intermediates on the acid sites of the HZSM-5 zeolite leads to the blockage of the pores due to their transformation into polyaromatic coke [49]. This effect is also named "overloading", and can be mitigated by diminishing the acid site density [50,51]. Hence, the reduction of the number of available sites due to the competitive nC_5 adsorption attenuates the rate of catalyst deactivation. Nonetheless, taking into account the adsorption heat values of methanol and nC_5, which were found to be ca. -115 [52] and ca. -62 kJ mol^{-1} [53], respectively, *n*-pentane adsorption will unlikely compete with that of methanol.

This suggests that a synergetic effect between the mechanisms of both reactants may be taking place. Arora et al. [54] reported the important role of H_2 co-fed with methanol at high pressure in the attenuation of coke formation. A nC_5 cracking-dominated mechanism would lead to a potential production of H_2 (through protolytic cracking), which could contribute to deactivation delay. However, the favored adsorption heat

values of methanol suggest that the overall mechanism should be dominated by the formation of methoxy species and a subsequent activation of the paraffin. Furthermore, the nC_5 conversion in **Figure 1** is in the 10% range, whereas full conversion of methanol and DME are found in most cases. All in all, the presence of H_2 should not be expected to play a key role in the catalyst stability despite it could be beneficial.

The direct participation of nC_5 on the dual cycle mechanism and then, on the formation and evolution of coke from oxygenates, could also explain the attenuation of deactivation. The relative contribution of the alkene and arene cycle depends on the catalyst properties and the reaction conditions [55]. A detailed evolution of the yields of products for the combined reactions of MeOH/nC_5 and DME/nC_5 are illustrated in **Figures S4** and **S5**, respectively. In addition, the same results are provided in **Figure S6** for the individual reactions at the partial pressure corresponding to an OX/nC_5 ratio of 0.25 (conditions of **Figure S3**). As expected, the increase in the OX/nC_5 ratio leads to higher yields of olefins, C_{5+} hydrocarbons and aromatics, whereas higher concentrations of nC_5 in the feed increases the yields of paraffins. This is related to the domination of the dual cycle mechanism of oxygenates when the OX/nC_5 ratio is high enough. The comparison of the results using an OX/nC_5 ratio in the feed of 0.25 with those of the individual reactions points out some interesting variations in the product distribution. The presence of nC_5 in the feed reduces the yields of ethylene from ca. 2.5 (MeOH) and ca. 7.5% (DME) to ca. 2% in the combined reactions, and the one of BTX aromatics from ca. 3 (MeOH) and ca. 6% (DME) to ca. 0.5 (MeOH) and ca. 1.5% (DME). Moreover, the production of C_{5+} hydrocarbons is almost suppressed in the combined reactions, from ca. 8 (MeOH) and ca. 20% (DME) in the individual reactions to ca. 1 (MeOH) and ca. 2% (DME) in the combined ones. This suggests that the presence of nC_5 could promote the cracking pathway of the alkene cycle in the dual cycle mechanism. Thus, the subsequent cyclization and aromatization of the alkene to coke species would be inhibited. The increase in the C_{2-3} saturated compounds from ca. 0.5 (MeOH and DME) in the individual reactions to ca. 6.5 (MeOH) and ca. 3.5% (DME) in the combined ones also suggests this promoted cracking pathway.

Figure 5 shows the evolution with time on stream of the O/P ratio for combined reactions of nC_5 with MeOH (**Figure 5a**) and DME (**Figure 5b**). This ratio can also give information about the relative contribution of each cycle during the conversion of MeOH/DME into olefins. The O/P ratio is slightly higher in the case of the individual

nC_5 reaction than that obtained in the combined reactions with MeOH/nC_5 ratio of 0.1 in the feed (**Figure 5a**). Nonetheless, the use of MeOH/nC_5 and DME/nC_5 (**Figure 5b**) ratios lower than 0.25 in the feed leads to stable values of O/P ratio and similar to the ones expected for the catalytic cracking of paraffins (cracking-dominated dual cycle mechanism). An increase in the OX/nC_5 molar ratio in the feed leads to a linear increase of the O/P ratio over time on stream. Zhang et al. [56] associated the increase in olefin production with a propagation of hydride transfer pathway that increases the contribution of the arene cycle of the dual-cycle mechanism. Then, the increase in the olefin selectivity should go in parallel with the formation of polyalkylaromatics and a faster deactivation. In contrast, low O/P ratios would suggest a higher contribution of the alkene cycle, observed with low OX/nC_5 and could explain the steady conversion of oxygenates over time on stream.

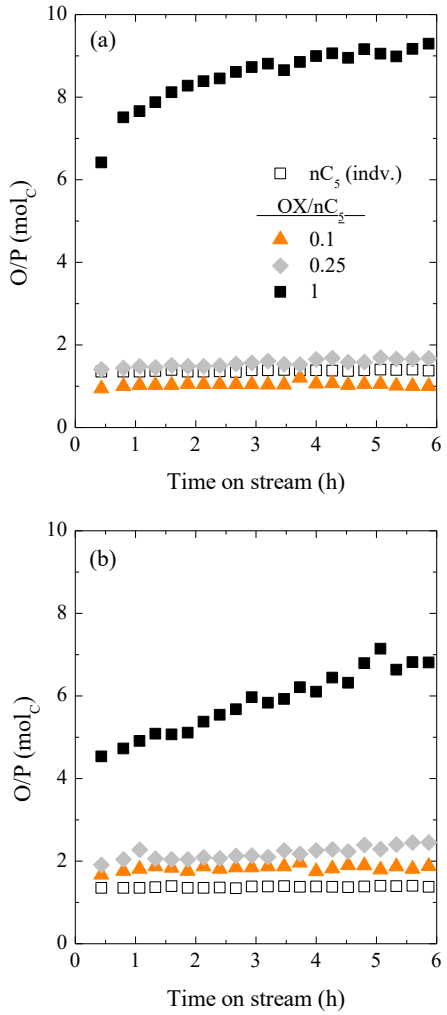

Figure 5. Evolution with time on stream of the olefin-to-paraffin ratio in combined reactions with different OX/nC_5 ratios using (a) MeOH and (b) DME in the feed (500 ºC, 1.0 $g_{catalyst}$ h mol_C^{-1})

Figure 6 schematizes the possible contribution of the nC_5 in the dual cycle mechanism of oxygenates (OX). As introduced by Bjørgen et al. [19], and later refined by other authors [57,58], the mechanism is based on the alkene and arene cycles in which the intermediates (I_{Alk} and I_{Ar}, respectively) are methylated, being both cycles interconnected by the hydrogen transfer pathway. Olefins (O) can be produced by the cracking of the I_{Alk} or the dealkylation of the I_{Ar}. At MTO conditions, the arene cycle is promoted, which maximizes the olefin production but also the formation of coke species (see **Figure 6**). According to our results at the optimal co-feeding conditions, nC_5 cracking could be promoting the cracking pathway of the alkene cycle, and then minimizing the formation of the arene cycle intermediates and their evolution to coke structures. The hydrogen transfer between the paraffin and the intermediates could be substituting the one between both cycles of the mechanism, while activating the cracking of the nC_5. This cooperative effect is also beneficial in energy terms, as the conversion of oxygenates is an exothermic step (red lines), whereas the cracking of paraffins is endothermic (blue lines).

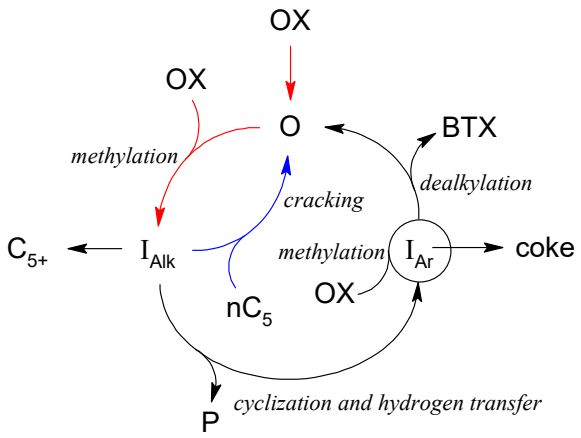

Figure 6. Proposed possible integration of the paraffin catalytic cracking into the dual cycle mechanism of oxygenates

A similar attenuating effect related to coke deposition and catalyst lifetime was previously reported for the combined reactions of bio-oil (a mixture of oxygenates and water) and vacuum gas oil (VGO, a mixture of hydrocarbons) [59,60]. In these cases, the lower coke deposition and its lighter nature were attributed to hydrogen transfer reactions between the hydrocarbons present in the VGO and the coke precursors, which reduce the rate of their evolution toward polyaromatic structures. Thus, the coke deposited during the combined reactions of nC_5 with oxygenates was investigated in order to analyze how these synergetic effects affect its formation.

After reaction, the catalysts were characterized by means of TG-TPO analysis. **Figure 7a** shows the TG-TPO profiles of the catalysts used in the combined reactions of nC_5 and MeOH. The content of coke increases upon increasing the MeOH/nC_5 ratio in the feed. Negligible values are registered for the individual reaction of nC_5 (0.2 wt%), and the combined reactions with MeOH/nC_5 ratios of 0.1 and 0.25 (0.6 and 0.8 wt%, respectively). However, the content of coke increases to 3.0 wt% when increasing the MeOH/nC_5 ratio up to 1, being 7.6 wt% the content of coke obtained in the individual reaction of MeOH. The promotion of coke formation is more evident when co-feeding DME instead of MeOH (**Figure 7b**), and values of 0.8, 2.1 and 9.3 wt% are registered for DME/nC_5 ratios in the feed of 0.1, 0.25 and 1, respectively. The maximum content of coke is registered for the individual reaction of DME, with a value of 16.8 wt%.

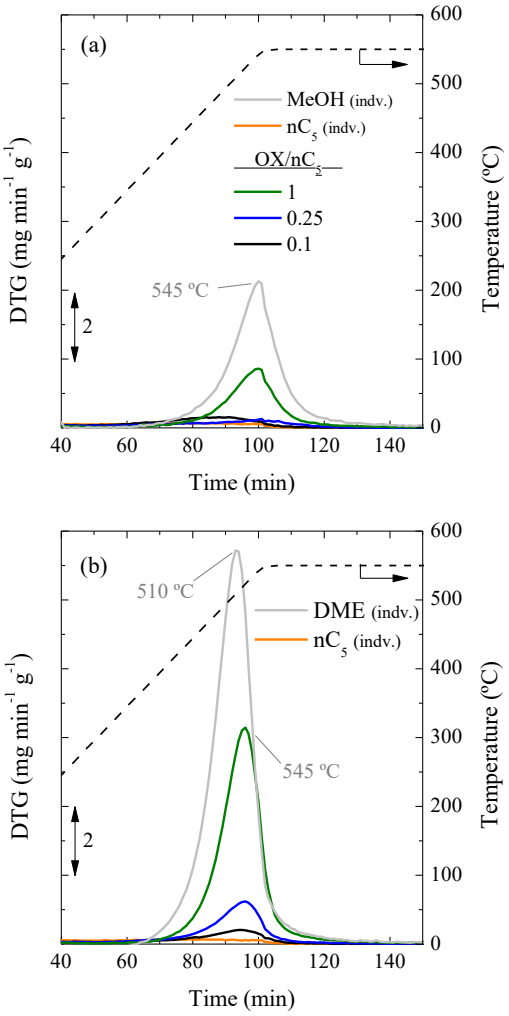

Figure 7. TPO profiles of used catalyst in the individual and combined reactions of nC_5 with different OX/nC_5 ratios in the feed using (a) MeOH and (b) DME (500 ºC, 1.0 $g_{catalyst}$ h mol_C^{-1})

In all cases, the peak attributed to the coke combustion is located at 545 ºC, except for the individual DME reaction. Besides presenting the maximum amount of coke, a shift towards a lower combustion temperature (510 ºC) is observed when the catalyst was used in the individual reaction of DME. The combustion temperature is usually attributed to the location and nature of coke. In this particular case, a massive deposition of coke was observed along the total catalytic bed (different axial positions). This experimental observation, along with the aforementioned formation of CO_x and CH_4, indicates that the deposition of coke is presumably taking place on the external surface of the γ–Al_2O_3 matrix of the catalyst [44]. A thermal experimental run using a

mesoporous γ-Al_2O_3 without zeolite confirms this hypothesis. **Figure S7** shows the TPO profile of this thermal run in which only CO_x and CH_4 are observed in the product stream. The TPO profile exhibits a neat peak located a 510 ºC, similar to that observed in **Figure 7b** for the DME individual reaction.

Aiming for a deep characterization of the physico-chemical properties of the used catalyst, the results of N_2 and tBA adsorption-desorption experiments are depicted in **Table S1**. The decrease in the specific surface areas (S_{BET}) is very low (maximum decrease, 32 m^2 g^{-1}) for the catalysts used in the individual nC_5 or combined reactions with OX/nC_5 of 0.1 or 0.25 in the feed. This result is consistent with the stability of the conversion registered for these reactions. In all these cases, as well as in the individual MeOH reaction, the drop of mesopore volume (V_{mes}) is not so high (**Table S1**). It is noteworthy that the low content of coke deposited on the catalyst used in the individual nC_5 reaction should be located within the zeolite crystals, thus leading to a decay of the micropore volume percentage. However, decreases in the external surface area (S_{ext}) are more significant in samples exposed to a reactant mixture with an OX/nC_5 molar ratio of 0.25. This suggests that at this point, coke from MeOH or DME starts depositing on the catalyst external surface of the mesoporous matrix [44,61]. Minimum values of S_{BET}, S_{ext} and V_{mes} are observed in the catalyst used in the individual reaction of DME. The result is in good agreement with the large coke deposition and the fast deactivation observed in this reaction. Similar trends are observed when correlating the coke content and the acidity of the used catalyst. A faster and more pronounced decay of the remaining acidity is observed upon increasing the amount of co-fed DME as compared to that of co-feeding MeOH.

The used catalysts were also characterized by means of confocal fluorescence microscopy (CFM), a technique used for the detection of different domains in a catalyst particle after an impregnation with fluorescent probe molecules [62]. Interestingly, some coke species such as conjugated dienes show autofluorescence under the applied laser conditions. **Figure 8a** shows the CFM image of a catalyst particle used in the individual nC_5 reaction. Clearly differentiated domains are observed with higher intensity than the main background of the particles that correspond to the zeolite crystals where the coke is primarily formed within the micropores [61]. This is consistent with the reduced V_{micr} and the preserved V_{mes} determined for this sample (**Table S1**). Nevertheless, the presence of a fluorescent background could be attributed

to the migration of some coke precursors from the crystals to the matrix previously observed in this kind of catalysts [44].

Figure 8b and **8c** display the CFM images collected for used catalysts in the individual reactions of MeOH and DME, respectively. Using the same brightness and contrast scales as in **Figure 8a**, negligible fluorescence is emitted by these two samples and only the reflection image is observed. This could presumably be caused by the higher amount of coke in these samples with a more developed nature, which has a relatively low florescence. In any case, it can be deduced that coke formed during the conversion of nC_5 and oxygenates is different in nature due to its refractoriness and/or chemical composition, being the former much more fluorescent.

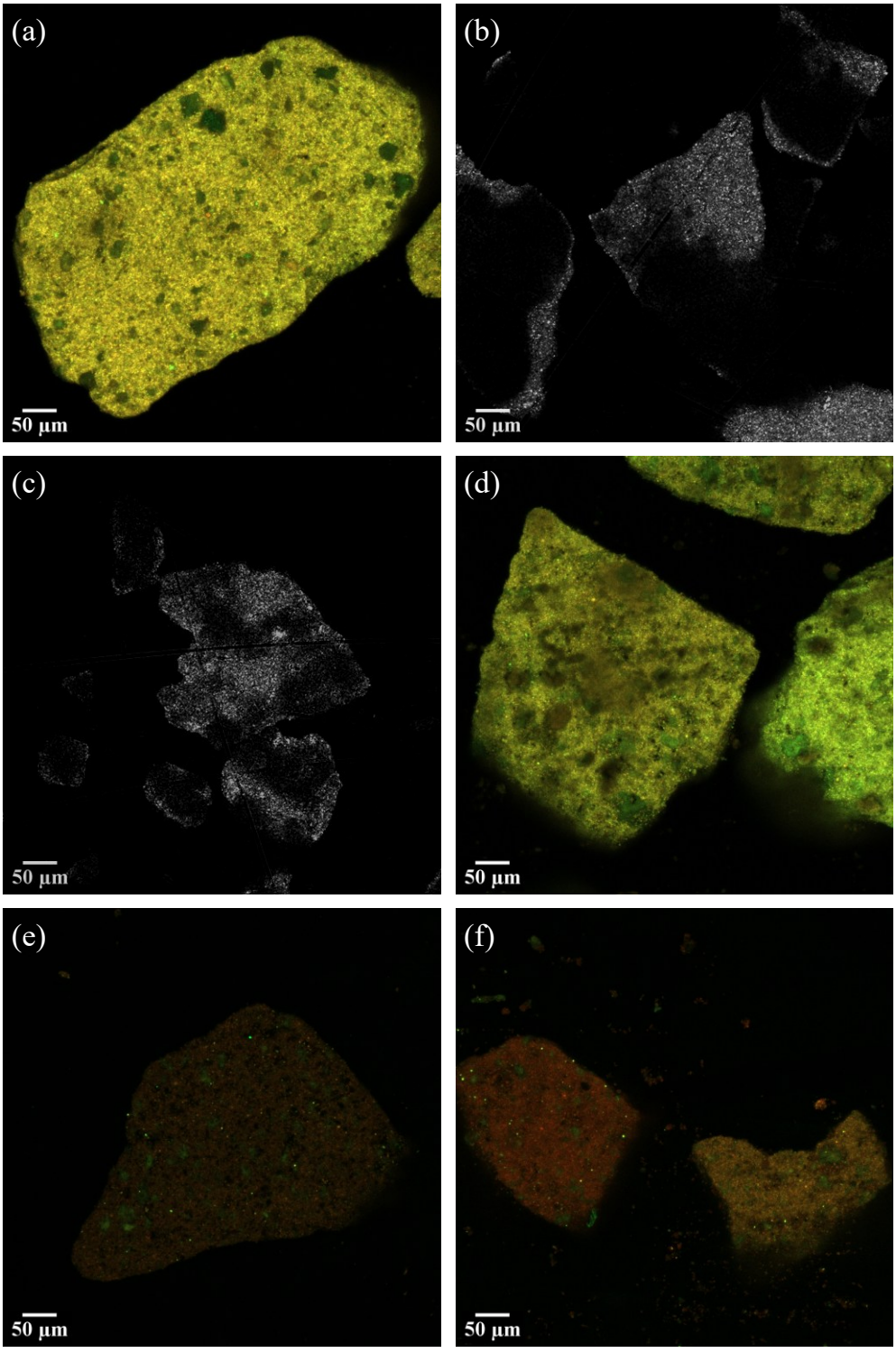

Figure 8. CFM images of used catalysts in the individual reactions of (a) nC_5, (b) MeOH and (c) DME and in the combined reactions of nC_5 and oxygenates with MeOH/nC_5 ratios of (d) 0.1 and (e) 1 and (f) with a DME/nC_5 ratio of 0.1 (500 ºC, 1.0 $g_{catalyst}$ h mol_C^{-1})

Interestingly, the OX/nC_5 in the feed and the used oxygenate (MeOH or DME) deeply affects the CFM images in **Figure 8**. First, the increase in the $MeOH/nC_5$ molar ratio from 0.1 to 1 leads to a significant decrease in the autofluorescence of the samples (**Figure 8d** and **8e**, respectively). This could be ascribed to a progressive change of the coke formation mechanism, with the one corresponding to MeOH acquiring more and more importance. The promotion of the arene cycle when increasing the MeOH content in the feed was previously discussed in section 3.1. This mechanism is the ultimate cause of coke formation in the dual cycle mechanism and presumably explains the loss of the fluorescence (coke from oxygenate). Secondly, the same amount of DME in the feed (DME/nC_5 of 0.1) causes a more pronounced autofluorescence reduction (**Figure 8f**), which also confirms the larger capacity of DME for promoting the mechanisms of coke formation as compared to MeOH.

4. Conclusions

A cooperation has been observed when performing the combined reactions of *n*-pentane cracking with methanol (MeOH) or dimethyl ether (DME) at 500 ºC in the presence of a high silica HZSM-5 zeolite catalyst (Si/Al = 140). In the optimum proportion of *n*-pentane and oxygenate, the individual reactions of each reactant are improved due to the combination of some steps of the different mechanism involved in the overall process.

The increase in *n*-pentane conversion for low amounts of MeOH or DME in the feed (OX/nC_5 molar ratios of 0.1 and 0.25) can be explained by the fast formation of methoxy and olefin intermediates from the oxygenated reactants, which would facilitate the initial activation of the alkane by hydrogen transfer reactions. Under these conditions, the interaction between the MeOH/DME dual cycle and paraffin cracking mechanisms could be explained by the easier formation and higher stability of the methoxy intermediates from the oxygenates as compared to that of the penta-coordinated carbonium ion formed by direct protonation of the *n*-paraffin. Especially, double *n*-pentane conversions and maximum selectivity of propylene are achieved using DME rather than MeOH. Our hypothesis is that it may be due to the higher reactivity of DME and the increased production of these methoxy intermediates. When higher amounts of oxygenates are co-fed, a decrease in the *n*-pentane conversion is observed.

During the conversion of MeOH/DME, a fast deactivation by coking occurs. The presence of *n*-pentane in the reaction medium significantly reduces the catalyst deactivation undergone during the individual MeOH or DME conversions, enlarging the catalyst lifetime. The experimental data suggests the participation of the paraffin in the coke formation pathways from oxygenates, by promoting the alkene cycle and then, limiting the extension of the arene one. This leads to a decrease in the concentration of polymethylbenzenes, the main coke precursors under the studied conditions. The analyses of the used catalyst by means of temperature-programmed oxidation and confocal fluorescence microscopy point out the higher deposition of coke using DME because of its higher reactivity than that of MeOH.

Our results are encouraging in order to acquire guidelines on the catalyst preparation and selection of the reaction conditions in such a way that the synergetic effects found in the combined reactions of paraffins and MeOH/DME can be potentiated. Then, they could be interesting for the intensification of olefin production in MTO/DTO processes, the valorization of oxygenates derived from biomass or the conversion of overproduced paraffins in conventional refinery units.

Acknowledgements

TC-L, ATA, PC and JB acknowledge the financial support received by the Spanish Ministry of Economy and Competitiveness with some ERDF funds (CTQ2016-77812-R, CTQ2016-79646-P), the Basque Government (IT1218-19) and the European Commission (HORIZON H2020-MSCA RISE-2018. Contract No. 823745). TC-L also acknowledges the Spanish Ministry of Education, Culture and Sport for the award of the FPU grant (FPU15-01666) and the additional mobility grant (EST17-00094). CM and AC acknowledge national and regional funding (MICINN/GVA) through 'Severo Ochoa" (SEV-2016-0683), RTI2018-101033-B-I00 and AICO/2019/060 and financial support from EU by ERC-AdG-2014-671093 (SynCatMatch) and from the Fundación Ramón Areces through a research contract of the "Life and Materials Science" program. The authors also thank Dr. Ricardo Andrade of the SGIker of UPV/EHU for the support provided with the CFM technique.

References

[1] S.M. Sadrameli, Thermal/catalytic cracking of liquid hydrocarbons for the production of olefins: A state-of-the-art review II: Catalytic cracking review, Fuel. 173 (2016) 102–115.

[2] S.M. Sadrameli, Thermal/catalytic cracking of liquid hydrocarbons for the production of olefins: A state-of-the-art review I: Thermal cracking review, Fuel. 140 (2015) 102–115.

[3] A. Corma, J. Mengual, P.J. Miguel, Stabilization of ZSM-5 zeolite catalysts for steam catalytic cracking of naphtha for production of propene and ethene, Appl. Catal. A Gen. 421–422 (2012) 121–134.

[4] X. Li, W. Li, F. Rezaei, A. Rownaghi, Catalytic cracking of n-hexane for producing light olefins on 3D-printed monoliths of MFI and FAU zeolites, Chem. Eng. J. 333 (2018) 545–553.

[5] J. Fu, X. Feng, Y. Liu, H. Shan, C. Yang, Mechanistic Insights into the Pore Confinement Effect on Bimolecular and Monomolecular Cracking Mechanisms of N -Octane over HY and HZSM-5 Zeolites: A DFT Study, J. Phys. Chem. C. 122 (2018) 12222–12230.

[6] A. Corma, J. Planelles, J. Sánchez-Marín, F. Tomás, The role of different types of acid site in the cracking of alkanes on zeolite catalysts, J. Catal. 93 (1985) 30–37.

[7] X. Hou, Y. Qiu, X. Zhang, G. Liu, Analysis of reaction pathways for n-pentane cracking over zeolites to produce light olefins, Chem. Eng. J. 307 (2017) 372–381.

[8] A. Corma, J. Mengual, P.J. Miguel, Steam catalytic cracking of naphtha over ZSM-5 zeolite for production of propene and ethene: Micro and macroscopic implications of the presence of steam, Appl. Catal. A Gen. 417–418 (2012) 220–235.

[9] A. Corma, J. Mengual, P.J. Miguel, IM-5 zeolite for steam catalytic cracking of naphtha to produce propene and ethene. An alternative to ZSM-5 zeolite, Appl. Catal. A Gen. 460–461 (2013) 106–115.

[10] A. Martin, S. Nowak, B. Lücke, H. Günschel, Coupled conversion of methanol and C4 hydrocarbons to lower olefins, Appl. Catal. 50 (1989) 149–155.

[11] B. Lücke, A. Martin, H. Günschel, S. Nowak, CMHC: coupled methanol hydrocarbon cracking, Microporous Mesoporous Mater. 29 (1999) 145–157.

[12] D. Mier, A.T. Aguayo, A.G. Gayubo, M. Olazar, J. Bilbao, Synergies in the production of olefins by combined cracking of n-butane and methanol on a HZSM-5 zeolite catalyst, Chem. Eng. J. 160 (2010) 760–769.

[13] S.M. Yu, J.F. Wu, C. Liu, W. Liu, S. Bai, J. Huang, W. Wang, Alkane activation initiated by hydride transfer: Co-conversion of propane and methanol over H-ZSM-5 Zeolite, Angew. Chem. Int. Ed. 54 (2015) 7363–7366.

[14] G. Roohollahi, M. Kazemeini, A. Mohammadrezaee, R. Golhosseini, The joint reaction of methanol and i-butane over the HZSM-5 zeolite, J. Ind. Eng. Chem. 19 (2013) 915–919.

[15] A. Kazemi, M. Beheshti, R. Khalili, Influence of recycle streams of C5/C6 and C4 hydrocarbon cuts on the performance of methanol to propylene (PVM) reactors, Chem. Eng. Sci. 172 (2017) 385–394.

[16] A. Corma, W. Wojciechowski, The Chemistry of catalytic crackin, Catal. Rev. Sci. Eng. 27 (1985) 29–150.

[17] A. Corma, P.J. Miguel, A. V. Orchillés, Product selectivity effects during cracking of alkanes at very short and longer times on stream, Appl. Catal. A Gen. 138 (1996) 57–73.

[18] A. Corma, A. V. Orchillés, Current views on the mechanism of catalytic cracking, Microporous Mesoporous Mater. 35–36 (2000) 21–30.

[19] M. Bjørgen, S. Svelle, F. Joensen, J. Nerlov, S. Kolboe, F. Bonino, L. Palumbo, S. Bordiga, U. Olsbye, Conversion of methanol to hydrocarbons over zeolite H-ZSM-5: On the origin of the olefinic species, J. Catal. 249 (2007) 195–207.

[20] F. Chang, Y. Wei, X. Liu, Y. Qi, D. Zhang, Y. He, Z. Liu, An improved catalytic cracking of n-hexane via methanol coupling reaction over HZSM-5 zeolite catalysts, Catal. Lett. 106 (2006) 171–176.

[21] S. Kotrel, H. Knözinger, B.C. Gates, The Haag-Dessau mechanism of protolytic cracking of alkanes, Microporous Mesoporous Mater. 35–36 (2000) 11–20.

[22] T. Cordero-Lanzac, A.T. Aguayo, A.G. Gayubo, P. Castaño, J. Bilbao,

Simultaneous modeling of the kinetics for n-pentane cracking and the deactivation of a HZSM-5 based catalyst, Chem. Eng. J. 331 (2018) 818–830.

[23] S. Wang, Y. Chen, Z. Qin, T.S. Zhao, S. Fan, M. Dong, J. Li, W. Fan, J. Wang, Origin and evolution of the initial hydrocarbon pool intermediates in the transition period for the conversion of methanol to olefins over H-ZSM-5 zeolite, J. Catal. 369 (2019) 382–395.

[24] C. Wang, J. Xu, G. Qi, Y. Gong, W. Wang, P. Gao, Q. Wang, N. Feng, X. Liu, F. Deng, Methylbenzene hydrocarbon pool in methanol-to-olefins conversion over zeolite H-ZSM-5, J. Catal. 332 (2015) 127–137.

[25] U. Olsbye, S. Svelle, K.P. Lillerud, Z.H. Wei, Y.Y. Chen, J.F. Li, J.G. Wang, W.B. Fan, The formation and degradation of active species during methanol conversion over protonated zeotype catalysts, Chem. Soc. Rev. 44 (2015) 7155–7176.

[26] J. Goetze, B.M. Weckhuysen, Spatiotemporal coke formation over zeolite ZSM-5 during the methanol-to-olefins process as studied with: Operando UV-vis spectroscopy: A comparison between H-ZSM-5 and Mg-ZSM-5, Catal. Sci. Technol. 8 (2018) 1632–1644.

[27] D. Rojo-Gama, M. Signorile, F. Bonino, S. Bordiga, U. Olsbye, K.P. Lillerud, P. Beato, S. Svelle, Structure–deactivation relationships in zeolites during the methanol–to-hydrocarbons reaction: Complementary assessments of the coke content, J. Catal. 351 (2017) 33–48.

[28] M. Boronat, A. Corma, What Is Measured When Measuring Acidity in Zeolites with Probe Molecules?, ACS Catal. 9 (2019) 1539–1548.

[29] J.S. Martinez-Espin, M. Mortén, T.V.W. Janssens, S. Svelle, P. Beato, U. Olsbye, New insights into catalyst deactivation and product distribution of zeolites in the methanol-to-hydrocarbons (MTH) reaction with methanol and dimethyl ether feeds, Catal. Sci. Technol. 7 (2017) 2700–2716.

[30] T.R. Forester, R.F. Howe, In situ FTIR studies of methanol and dimethyl ether in ZSM-5, J. Am. Chem. Soc. 109 (1986) 5076–5082.

[31] H. Yamazaki, H. Shima, H. Imai, T. Yokoi, T. Tatsumi, J.N. Kondo, Direct production of propene from methoxy species and dimethyl ether over H-ZSM-5,

J. Phys. Chem. C. 116 (2012) 24091–24097.

[32] J. Li, Z. Wei, Y. Chen, B. Jing, Y. He, M. Dong, H. Jiao, X. Li, Z. Qin, J. Wang, W. Fan, A route to form initial hydrocarbon pool species in methanol conversion to olefins over zeolites, J. Catal. 317 (2014) 277–283.

[33] J.S. Martinez-Espin, K. De Wispelaere, M. Westgård Erichsen, S. Svelle, T.V.W. Janssens, V. Van Speybroeck, P. Beato, U. Olsbye, Benzene co-reaction with methanol and dimethyl ether over zeolite and zeotype catalysts: Evidence of parallel reaction paths to toluene and diphenylmethane, J. Catal. 349 (2017) 136–148.

[34] P. Pérez-Uriarte, M. Gamero, A. Ateka, M. Díaz, A.T. Aguayo, J. Bilbao, Effect of the acidity of HZSM-5 zeolite and the binder in the DME transformation to olefins, Ind. Eng. Chem. Res. 55 (2016) 1513–1521.

[35] S. Svelle, F. Joensen, J. Nerlov, U. Olsbye, K.P. Lillerud, S. Kolboe, M. Bjørgen, Conversion of methanol into hydrocarbons over zeolite H-ZSM-5: Ethene formation is mechanistically separated from the formation of higher alkenes, J. Am. Chem. Soc. 128 (2006) 14770–14771.

[36] W.O. Haag, R.M. Dessau, Proceedings 8th International Congress on Catalysis, Berlin, Vol. 2, Proceedings 8th International Congress on Catalysis, Berlin, Vol. 2, 1984.

[37] M. Boronat, P.M. Viruela, A. Corma, Reaction Intermediates in Acid Catalysis by Zeolites: Prediction of the Relative Tendency to Form Alkoxides or Carbocations as a Function of Hydrocarbon Nature and Active Site Structure, J. Am. Chem. Soc. 126 (2004) 3300–3309.

[38] Y. Jiang, M. Hunger, W. Wang, On the Reactivity of Surface Methoxy Species in Acidic Zeolites, J. Am. Chem. Soc. 128 (2006) 11679–11692.

[39] P. Pérez-Uriarte, A. Ateka, A.G. Gayubo, T. Cordero-Lanzac, A.T. Aguayo, J. Bilbao, Deactivation kinetics for the conversion of dimethyl ether to olefins over a HZSM-5 zeolite catalyst, Chem. Eng. J. 311 (2017) 367–377.

[40] Y. Liu, F.M. Kirchberger, S. Müller, M. Eder, M. Tonigold, M. Sanchez-Sanchez, J.A. Lercher, Critical role of formaldehyde during methanol conversion to hydrocarbons, Nat. Commun. 10 (2019) 1–9.

[41] A. Hwang, A. Bhan, Deactivation of Zeolites and Zeotypes in Methanol-to-Hydrocarbons Catalysis: Mechanisms and Circumvention, Acc. Chem. Res. 52 (2019) 2647–2656.

[42] N.N. Ezhova, N. V. Kolesnichenko, T.I. Batova, Zeolite Catalysts for the Synthesis of Lower Olefins from Dimethyl Ether (a Review), Pet. Chem. 60 (2020) 459–470.

[43] K. De Wispelaere, C.S. Wondergem, B. Ensing, K. Hemelsoet, E.J. Meijer, B.M. Weckhuysen, V. Van Speybroeck, J. Ruiz-Martínez, Insight into the Effect of Water on the Methanol-to-Olefins Conversion in H-SAPO-34 from Molecular Simulations and in Situ Microspectroscopy, ACS Catal. 6 (2016) 1991–2002.

[44] T. Cordero-Lanzac, A. Ateka, P. Pérez-Uriarte, P. Castaño, A.T. Aguayo, J. Bilbao, Insight into the deactivation and regeneration of HZSM-5 zeolite catalysts in the conversion of dimethyl ether to olefins, Ind. Eng. Chem. Res. 57 (2018) 13689–13702.

[45] D. Chen, K. Moljord, T. Fuglerud, A. Holmen, The effect of crystal size of SAPO-34 on the selectivity and deactivation of the MTO reaction, Microporous Mesoporous Mater. 29 (1999) 191–203.

[46] D. Chen, K. Moljord, A. Holmen, A methanol to olefins review: Diffusion, coke formation and deactivation on SAPO type catalysts, Microporous Mesoporous Mater. 164 (2012) 239–250.

[47] Y. Li, M. Zhang, D. Wang, F. Wei, Y. Wang, Differences in the methanol-to-olefins reaction catalyzed by SAPO-34 with dimethyl ether as reactant, J. Catal. 311 (2014) 281–287.

[48] C. Li, A. Vidal-Moya, P.J. Miguel, J. Dedecek, M. Boronat, A. Corma, Selective Introduction of Acid Sites in Different Confined Positions in ZSM-5 and Its Catalytic Implications, ACS Catal. 8 (2018) 7688–7697.

[49] J. Valecillos, E. Epelde, J. Albo, A.T. Aguayo, J. Bilbao, P. Castaño, Slowing down the deactivation of H-ZSM-5 zeolite catalyst in the methanol-to-olefin (MTO) reaction by P or Zn modifications, Catal. Today. 348 (2020) 243–256.

[50] L. Qi, J. Li, L. Wang, L. Xu, Z. Liu, Unusual deactivation of HZSM-5 zeolite in the methanol to hydrocarbon reaction, Catal. Sci. Technol. 7 (2017) 894–901.

[51] L. Qi, J. Li, L. Wang, C. Wang, L. Xu, Z. Liu, Comparative investigation of the deactivation behaviors over HZSM-5 and HSAPO-34 catalysts during low-temperature methanol conversion, Catal. Sci. Technol. 7 (2017) 2022–2031.

[52] S. Ilias, A. Bhan, Mechanism of the catalytic conversion of methanol to hydrocarbons, ACS Catal. 3 (2013) 18–31.

[53] S. Schallmoser, T. Ikuno, M.F. Wagenhofer, R. Kolvenbach, G.L. Haller, M. Sanchez-Sanchez, J.A. Lercher, Impact of the local environment of Bronsted acid sites in ZSM-5 on the catalytic activity in n-pentane cracking, J. Catal. 316 (2014) 93–102.

[54] S.S. Arora, Z. Shi, A. Bhan, Mechanistic Basis for Effects of High-Pressure H2 Cofeeds on Methanol-to-Hydrocarbons Catalysis over Zeolites, ACS Catal. 9 (2019) 6407–6414.

[55] T.V.W. Janssens, S. Svelle, U. Olsbye, Kinetic modeling of deactivation profiles in the methanol-to-hydrocarbons (MTH) reaction: A combined autocatalytic-hydrocarbon pool approach, J. Catal. 308 (2013) 122–130.

[56] M. Zhang, S. Xu, Y. Wei, J. Li, J. Wang, W. Zhang, S. Gao, Z. Liu, Changing the balance of the MTO reaction dual-cycle mechanism: Reactions over ZSM-5 with varying contact times, Cuihua Xuebao/Chinese J. Catal. 37 (2016) 1413–1422.

[57] A.D. Chowdhury, K. Houben, G.T. Whiting, M. Mokhtar, A.M. Asiri, S.A. Al-Thabaiti, M. Baldus, B.M. Weckhuysen, Initial Carbon–Carbon Bond Formation during the Early Stages of the Methanol-to-Olefin Process Proven by Zeolite-Trapped Acetate and Methyl Acetate, Angew. Chem. Int. Ed. 55 (2016) 1–7.

[58] V. Van Speybroeck, K. De Wispelaere, J. Van Der Mynsbrugge, M. Vandichel, K. Hemelsoet, M. Waroquier, First principle chemical kinetics in zeolites: The methanol-to-olefin process as a case study, Chem. Soc. Rev. 43 (2014) 7326–7357.

[59] A. Ibarra, A. Veloso, J. Bilbao, J.M. Arandes, P. Castaño, Dual coke deactivation pathways during the catalytic cracking of raw bio-oil and vacuum gasoil in FCC conditions, Appl. Catal. B Environ. 182 (2015) 336–346.

[60] C. Wang, R. Venderbosch, Y. Fang, Co-processing of crude and hydrotreated pyrolysis liquids and VGO in a pilot scale FCC riser setup, Fuel Process.

Technol. 181 (2018) 157–165.

[61] M. Ibañez, P. Pérez-Uriarte, M. Sánchez-Contador, T. Cordero-Lanzac, A.T. Aguayo, J. Bilbao, P. Castaño, Nature and location of carbonaceous species in a composite HZSM-5 zeolite catalyst during the conversion of dimethyl ether into light olefins, Catalysts. 7 (2017) 254–266.

[62] G.T. Whiting, F. Meirer, M.M. Mertens, A.-J. Bons, B.M. Weiss, P.A. Stevens, E. de Smit, B.M. Weckhuysen, Binder Effects in SiO2- and Al2O3-Bound Zeolite ZSM-5-Based Extrudates as Studied by Microspectroscopy, ChemCatChem. 7 (2015) 1312–1321.